



OPEN

Transgenic expression of the N525S-tuberin variant in *Tsc2* mutant (Eker) rats causes dominant embryonic lethality

SUBJECT AREAS:
CANCER MODELS
TUMOUR SUPPRESSORSReceived
7 April 2014Accepted
19 June 2014Published
4 August 2014Correspondence and
requests for materials
should be addressed to
O.H. (ohino@med.
juntendo.ac.jp)Masatoshi Shiono^{1,2}, Toshiyuki Kobayashi², Riichi Takahashi^{3,4}, Masatsugu Ueda^{3,5}, Chikashi Ishioka^{1,6} & Okio Hino²

¹Department of Clinical Oncology, Tohoku University Hospital, Tohoku University, 1-1 Seiryomachi, Aoba-ku, Sendai, Miyagi 980-8574, Japan, ²Department of Pathology and Oncology, Juntendo University School of Medicine, 2-1-1 Hongo, Bunkyo-ku, Tokyo 113-8421, Japan, ³PhoenixBio Co., Ltd., 1198-4 Iwazomachi, Utsunomiya, Tochigi 321-0973, Japan, ⁴Animal Resources Center, Central Institute for Experimental Animals, 3-25-12 Tonomachi, Kawasaki, Kanagawa 210-0821, Japan, ⁵Transgenic Animal Division, Utsunomiya Institute, Institute of Immunology Co., Ltd., 1198-4 Iwazomachi, Utsunomiya, Tochigi 321-0973, Japan, ⁶Department of Clinical Oncology, Institute of Development, Aging, and Cancer, Tohoku University, 4-1 Seiryomachi, Aoba-ku, Sendai, Miyagi 980-8575, Japan.

The *Tsc2* product, tuberin, negatively regulates the mTOR pathway. We have exploited the Eker (*Tsc2*-mutant) rat system to analyse various *Tsc2* mutations. Here, we focus on the N525S-*Tsc2* variant (NSM), which is known to cause distinct symptoms in patients even though normal suppression of mTOR is observed. Unexpectedly, we were repeatedly unable to generate viable rats carrying the NSM transgene. Genotypic analysis revealed that most of the embryos carrying the transgene died around embryonic day after 14.5—similar to the stage of lethality observed for Eker homozygotes. Thus, the NSM transgene appeared to have a dominant lethal effect in our rat model. Further, no significant differences were observed for various signal transduction molecules in transiently expressed NSM cells compared to WT. These results indicate that a non-mTOR pathway, critical for embryogenesis, is being regulated by tuberin, providing a link between tuberin expression and the severity of *Tsc2* mutation-related pathogenesis.

Tuberous sclerosis (TSC) is an inherited autosomal dominant disease characterised by skin lesions (hamartomas), central nervous system disorders (e.g., cerebral tubera, seizures, and mental retardation), and systemic multiple tumoral lesions (e.g. subependymal giant cell astrocytoma of brain, angiomyolipoma of kidney and liver, rhabdomyoma of heart, lymphangioliomyomatosis of lung, retinal hamartoma, and angiofibroma) with an estimated prevalence of 1/6000¹. The two tumour suppressor genes responsible for TSC, *TSC1* (9q34), and *TSC2* (16p13.3) have been identified and positionally cloned^{2,3}. It is known that the protein products of *TSC1* (hamartin) and *TSC2* (tuberin) form a complex that exhibits GTPase-activating protein (GAP) function, converting Rheb, a small G protein located upstream of mTOR, into its inactive state^{4,5}. This function results in the downregulation of the mTOR-S6K1 pathway (mTOR-axis)^{6,7}.

Further, analysis of familial TSC patients has indicated that the clinical symptoms may be dependent on the particular mutations/variations of tuberin^{8–11}. Numerous mutations/variations exist in the *TSC2* gene, many of which have been reported to cause unusual mild symptoms^{12,13}. Here, we have focused on two missense mutations that seemed to be correlated to the severity of symptoms and mTOR-axis regulation. Although the human G1556S mutation (GSM) in tuberin is located within the GAP-related domain and affects Rheb-GAP activity, patients carrying this mutation display mild symptoms, such as normal brain imaging, skin lesions, and only the occasional hamartoma on other tissues^{14,15}. In contrast, the human N525S variant (NSM) in tuberin retains its Rheb-GAP activity, but the clinical manifestation of this variation is much more distinct, including cortical tubers, subependymal giant cell astrocytomas, renal angiomyolipomas, and cardiac rhabdomyomas^{8,14,16,17}. Thus, the status of the mTOR-axis does not correlate with symptom severity in patients with these mutations, suggesting that the aberrant activation of the mTOR-axis, although it may play a major role, is not the sole determinant of TSC pathogenesis. Additional studies on GSM, NSM, and other tuberin variants, with emphasis



Table 1 Generation of transgenic founder rats				
Summary of injection				
Gene	Number of			
	Injected eggs	Transferred eggs	Born offspring	Tg(+) rats
pMGTsc2-GSM (G1556S-type)	135	127	53	5 4(Tsc2+/+) 1(Tsc2+/-)
pMGTsc2-NSM (N525S-type)	236	214	73	0
pMGTsc2-WT (Wild-type)	172	106	21	5 1(Tsc2+/+) 4(Tsc2+/-)

*Donor animals: Eker(Tsc2+/-) ♂ × Wistar(Tsc2+/+).
[†]Phenotype of rats carrying GSM- or WT-Tg were previously reported²³.

on the *in vivo* mechanisms of action, are necessary in order to identify the novel pathways involved in the development of TSC as well as new therapeutic targets.

Importantly, a homolog of human *TSC2* (*Tsc2*) in the Eker rat, first shown to develop hereditary renal cancer naturally in 1953¹⁸, appears to be the gene responsible for this phenotype, making this animal model ideal for studying *Tsc2* function^{19–21}. Rats heterozygous for *Tsc2* develop renal tumours by one year of age without exception and homozygotes are embryonic lethal. In a previous study, we generated transgenic Eker rats carrying the cDNA and promoter of wild-type rat *Tsc2*, and demonstrated that the transgene (Tg) inhibited both renal carcinogenesis in Eker heterozygotes and embryonic lethality in homozygotes²². Further, Eker rats carrying the GSM-tuberin variant also had suppressed tumour formation, even though the mTOR pathway was disrupted²³. These data are consistent with the observation that patients carrying the GSM develop mild symptoms, suggesting that there is another pathway that regulates tumour progression, independent of the mTOR pathway. Correspondingly, we hypothesise that transgenic Eker rats carrying the NSM might develop severe tumorigenic phenotypes, albeit while retaining normal mTOR function, and thus, could provide a clue to uncover the novel function of *Tsc2* related to tumour progression. To investigate this possibility, we have exploited the transgenic Eker rat system to express the NSM and subsequently characterised tuberlin function and pathogenesis *in vivo*. In this analysis, both the wild-type- (WT-) and NSM-tuberin showed no difference in complex formation with hamartin, subcellular localisation, phosphorylation status, or mTOR inhibition *in vitro*. However, much to our surprise, we were unable to repeatedly generate viable newborn rats carrying the NSM Tg. In this study, we report an unexpected dominant effect of NSM-tuberin on development and cell growth.

Results

Our previous *in vitro* analyses showed that GSM-tuberin exhibited a change in the subcellular localisation (scattered throughout the cytosol), a weak interaction with hamartin, an altered phosphorylation status, and did not stimulate Rheb-GTPase activity or inhibit S6K and S6 phosphorylation^{15,16,23}. In contrast, NSM-tuberin had characteristics similar to the WT-tuberin with regard to subcellular localisation (forming the perinuclear dense bodies; PNDs), complex formation with hamartin at the PNDs, phosphorylation status, and Rheb-GTPase activity (intact) along with S6K and S6 phosphorylation^{14,16,17,23}.

To further investigate the function of these tuberlin mutants *in vivo* using our transgenic Eker rat system^{22–24}, we constructed Tgs for the expression of GSM- or NSM-tuberin (GSM Tg or NSM Tg, respectively). Our characterisation of the WT and GSM Tg rats has been reported previously²³. Despite repeated attempts, we were unable to generate viable newborn rats carrying the NSM Tg (Table 1). This

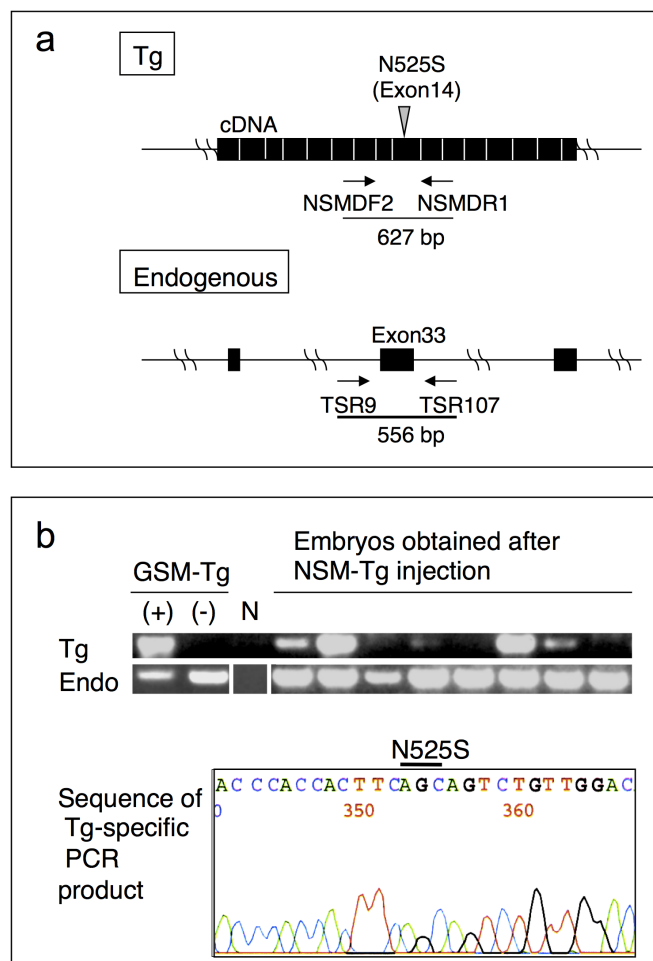


Figure 1 | Detection of NSM Tg-positive embryos. (a) Schematic diagram of the primers utilised for the Tg-specific and endogenous *Tsc2*-specific PCRs. Each filled box denotes the exon. (b) PCR genotyping results and sequencing analyses. Upper panel shows the PCR analysis of eight individual E10.5 embryos. DNAs from GSM Tg carrying (+) or non-carrying (-) rats were used as controls. Lane N indicates the template DNA negative control. Endogenous *Tsc2* was amplified as the PCR control (Endo). The blots have been cropped focusing on the bands of interest; See Supplementary Fig. S1 for full-length gels. Lower panel shows the sequence of the Tg-specific PCR product. The position of the N525S mutation is indicated.

result was unexpected as the *in vitro* characteristics of NSM-tuberin were similar to those of WT-tuberin^{8,14,16,17}. We therefore screened embryos at different stages of gestation following injection of NSM Tg DNA. At embryonic day (E) 10.5, Tg-positive embryos were detected using Tg-specific PCR genotyping (Fig. 1a) and the inserted sequence was confirmed to be that of the NSM Tg (Fig. 1b). Then, we proceeded to determine the stage at which embryos carrying the NSM Tg die. The Eker homozygous condition is known to be lethal from day 13 to 18 of gestation^{25,26}. Intriguingly, the frequency of live NSM Tg-positive embryos fell abruptly after the E14.5 stage, suggesting that many of the NSM Tg-positive embryos died during this stage²⁶ (Table 2). The similarity in the timing of embryonic lethality in homozygous *Tsc2*^{Eker/Eker} mutants and NSM Tg carrying embryos might indicate that NSM-tuberin exerts a dominant negative effect on WT-tuberin function during embryonic rat development.

In order to further investigate the effects of NSM-tuberin, we tried to generate cell lines that stably expressed NSM *in vitro*. This type of methodology has been employed previously for WT-tuberin and, as NSM-tuberin exhibited similar characteristics to the WT construct



	Tg(+) embryos	Live embryos	Rate: Tg(+)/total
E10.5	11	22	0.500
E12.5	9	30	0.300
E14.5	6	22	0.273
E16.5	1	10	0.100
E18.5	2	16	0.125

in various transient expression experiments²³, expression was expected to result in similar phenotypic changes. Notably, since the aforementioned results indicated that stable expression of NSM-tuberin was predicted to exert some toxic cellular effects, we adopted a conditional gene expression system. However, despite our repeated attempts and changes to the tetracycline inducible expression system (RevTet-off System and Tet-On 3G System; Clontech, CA, USA) and the flow cytometry-based purification by tagged ZsGreen (with drug selection), none of these resulted in stable expression of NSM. In contrast, stable cell line expression of WT and GSM was successful (Fig. 2a–c). Therefore, we suspect that the NSM-tuberin has a dominant negative effect when it is constitutively expressed *in vivo* and *in vitro*.

To elucidate the mechanism of this putative dominant negative effect, we operated a series of additional *in vivo* (foetal tissue analysis) and *in vitro* (global analysis in major signal transduction pathways) analyses. In the tissue analysis, we observed no gross abnormalities or changes in individual embryo size at any stage irrespective of their NSM Tg genetic status (Fig. 3a). After examining sectioned embryonic NSM Tg positive tissues, exencephaly, which is frequently associated with lethality in Eker homozygotes and *Tsc1/2* knockout embryos^{25–28}, was not observed (Fig. 3b). In order to better understand this discrepancy in regards to the underlying mechanism, we performed a comprehensive analysis involving a variety of signal transduction molecules using transient expression cell lysates (Fig. 4a), whereby the relative tyrosine phosphorylation statuses of 44 different receptor tyrosine kinases (RTKs) were determined. Yet, no prominent difference was detected among the samples expressing control vector, WT-, or NSM-Tsc2 (Fig. 4b). In the Reverse Phase Protein Array (RPPA) analysis, 180 targets of the anti-phospho antibodies were also examined. However, the results among samples showed no distinct differences (Fig. 4c). Thus, no prominent difference was detected in any of the comprehensive analyses we adopted. Although further analyses are needed to elucidate the mechanism of these putative dominant negative effects, our data suggest the existence of a novel unknown pathway(s) that is, at least in part, regulated by NSM-tuberin *in vitro* and *in vivo*.

Discussion

mTOR is one of the major clinical therapeutic targets against cancer^{29–31}. While mTOR inhibitors are prescribed to treat various tumours^{32–36}, mTOR itself also serves as a major target in T cell suppression for transplantation and autoimmune disease^{37–39}. In a recent clinical trial, the oral mTOR inhibitor everolimus (rapamycin analogue) showed a marked 50% reduction in the subependymal giant cell astrocytoma (SEGA) volume in 32% of the TSC patients monitored⁴⁰. Although this outcome is encouraging, this everolimus monotherapy was not effective in the other 68% of patients, suggesting that solely using an mTOR inhibitor is not sufficient to cure TSC. To address this issue, it is urgent that we investigate the existence of any unknown critical pathways, beyond the mTOR pathway, related to TSC pathogenesis in order to develop more successful therapeutic targets.

In many reports, NSM-tuberin showed similar characteristics to the WT-tuberin in various transient expression experiments^{14,16,17}; however, the clinical manifestation of this variant in human patients

is severe. Therefore, the possibility that TSC may, in some cases, develop independently of mTOR hyper-activation has been raised¹⁷. It is possible that other unknown functional defects in tuberin may be resulting in the severe disease phenotype, which may explain the unexpected embryonic lethality induced by the NSM Tg that we observed in this study in rats. Our analysis indicates that the majority of NSM Tg-carrying embryos died after E14.5, corresponding with the time period for the highest incidence of embryonic deaths in Eker homozygous mutant embryos^{25,26}. Since we constructed the Tg using the intrinsic promoter of the wild-type *Tsc2*, it is possible that NSM expression is being induced in a spatiotemporally identical manner to endogenous *Tsc2* and the putative dominant negative effect against the endogenous *Tsc2* is occurring at the specific embryonic developmental stage when the gene begins to function. In regards to the similarity between the times of embryonic death for the two genotypes, we suggest that NSM affects normal embryonic development by generating a dominant negative effect in a pathway in which WT-tuberin has a function.

Furthermore, as there are human TSC patients with the N525S variation, we speculate that higher expression of the Tg compared to the endogenous gene may be required to exert the dominant-lethal effect when the wild-type *Tsc2* allele is present. Theoretically, in TSC patients with endogenous *TSC2* expression, the dominant negative function of N525S-tuberin could be elicited by inactivation of the wild-type *TSC2* allele and would be expected to induce severe symptoms. N525S has been suggested to be either a polymorphism⁴¹ or a mutation^{8,14,16,17}. Whichever is correct, it is certain that any type of variation in the *TSC* genes is likely playing a major role, potentially as a genetic modifier allele, in the susceptibility and phenotypic manifestation of the TSC-related disorders⁴². Hence, elucidation of the mechanism underlying the NSM-associated embryonic lethality at this stage of development will lead to the identification of a novel function of tuberin.

Here, we have demonstrated that NSM overexpression in rats causes embryonic lethality. Importantly, the N525S-type tuberin variant showed completely normal function when transiently expressed *in vitro* in regards to subcellular localisation, interaction with hamartin, phosphorylation, and mTOR regulation as compared to WT-tuberin. However, this variant also displayed a severe phenotype when stably expressed *in vitro* and *in vivo* (rats). To the best of our knowledge, this correlation between the function of tuberin and the severity of symptoms is completely novel and the elucidation of the unknown pathway through which NSM-tuberin functions will help to clarify the overall mechanism of TSC pathogenesis.

Methods

Plasmid construction. Schematic structures of the *Tsc2* transgene have been shown previously²³. Generation of GSM and NSM rat *Tsc2* cDNAs and construction of the pCAG-FLAG-rTsc2-GSM and pCAG-FLAG-rTsc2-NSM plasmids were also reported previously²³. NSM cDNA was used to replace the normal sequences in pMGTsc2-WT (the wild-type Tg used previously) in order to generate pMGTsc2-NSM. For the Tet-inducible systems, *Tsc2* cDNAs were cloned into pRev-TRE or pTRE3G-ZsGreen vectors (Clontech, CA, USA).

Microinjection and generation of transgenic founders. Wistar female rats (Purchased from Charles River Laboratories, Kanagawa, Japan) were injected intraperitoneally with hormone to stimulate ovulation and then mated with male Eker rats heterozygous for the *Tsc2* mutation. Fertilised eggs at the pronuclear stage were collected from impregnated females. Tg DNAs were linearised with *NotI*, purified using a QIAquick kit (QIAGEN, Hilden, Germany), and microinjected into the fertilised eggs⁴³. The eggs were then transferred into the oviducts of pseudo-pregnant Wistar females.

Genotyping. DNA was prepared from adult tails or embryonic tissues (whole embryo, placenta, or yolk sac) by proteinase K digestion and phenol extraction. For Southern blot analysis, 10 µg of DNA was digested with *BamHI*, subjected to 1% agarose gel electrophoresis, transferred onto a nylon membrane, and hybridised as described previously²¹. An *EcoRI-BamHI* rat *Tsc2* cDNA fragment covering exons 26–33 (1.1 kb) was used as a probe after ³²P-labelling. Genotyping by PCR was performed using the following primers: for endogenous *Tsc2*, TSR9 (5'-GCTTGTGCCTCT-AACAGTG-3', forward, intron 32) and TSR107 (5'-GCAACTGGGGTTTGTGC-

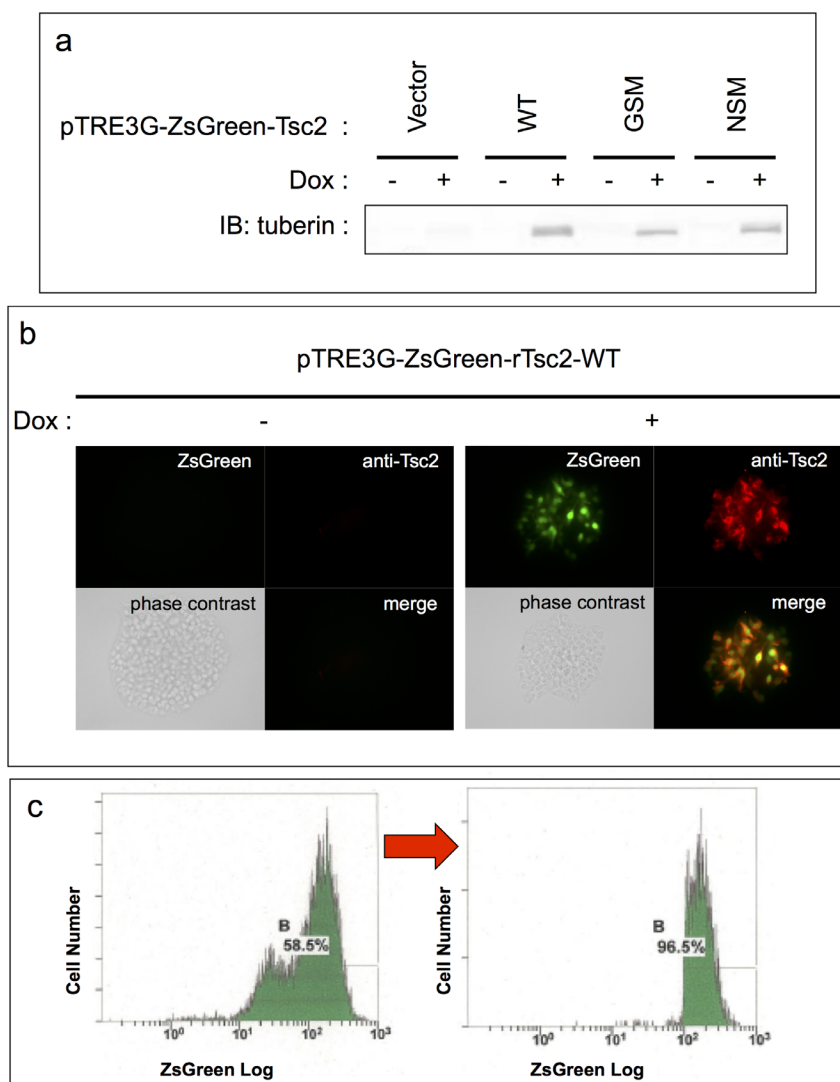


Figure 2 | Multiple attempts were made to establish cell lines stably expressing NSM-tuberin. (a) Tetracycline regulated the expression of each tuberin variant using Tet-on 3G system in HEK293 Tet-On 3G cells. Expression of each tuberin variant was appropriately induced by the presence or absence of doxycycline (Dox). Note that the previously reported band shift of GSM-tuberin compared to WT- or NSM-tuberin band was reproducible^{15,23}, suggesting that the system is working properly. The blots have been cropped, focusing on the bands of interest; See Supplementary Fig. S2 for full-length blots. (b) Tetracycline regulated the expression of each tuberin variant and ZsGreen using Tet-on 3G system in HEK293 Tet-On 3G cells. Representative immunofluorescent images are shown. Simultaneous tuberin variant and ZsGreen expression utilising IRES sequence was properly regulated by the presence or absence of Dox. (c) Representative flow cytometry (FCM) data showing the purification of ZsGreen-positive cells. The horizontal and vertical axes show the logarithmic fluorescent intensity and the number of cells, respectively. The percentages of the total live cells that were positive for ZsGreen are shown in each panel. Left panel; FCM before cell sorting (drug selection only). Although most cells are ZsGreen-positive, there are two peaks of cells in fluorescent intensity. To solve this heterogeneity in fluorescent intensity (indicating variable translational efficiency), cells were subjected to cell sorting. Right panel; FCM after cell sorting by gating stronger-ZsGreen-intensity peak. Subgroups of cells with weaker ZsGreen intensity (left peak in the left panel) were eliminated and subgroups with stronger ZsGreen intensity (right peak in the left panel) were purified by cell sorting. Cell lines stably expressing WT- and GSM-tuberin were successfully cultured, but despite numerous improvements in the methodology, cell lines that stably express NSM-tuberin were not obtained.

C-3', reverse, intron 33); and for NSM, NSMDF2 (5'-AGTTCACGGATCGCA-AGA-3', forward, exon 11) and NSMDR1 (5'-TAGCAATGGGCAAGGAGTAG-3', reverse, exon 16). The PCR amplification was performed using 35 cycles at 94°C for 1 min, 55°C for 1 min, and 72°C for 1.5 min.

Cell culture and transfection for transient expression. HEK293 cells were plated in collagen-coated 6-well plates at a density of 5×10^4 cells/well and cultured in Dulbecco's modified Eagle's medium supplemented with 10% foetal bovine serum (FBS) and penicillin/streptomycin. One day after plating, the HEK293 cells were transfected with plasmids (0.5 μ g each) using FuGENE6 (Roche, Mannheim, Germany) according to the manufacturer's instructions. Cells were analysed after incubating 48 h.

Tetracycline (Tet) inducible expression system. The RevTet-off System or Tet-On 3G System were exploited to establish Tet-off or Tet-on cell lines, respectively,

according to the manufacturer's instructions provided with the kits (Clontech, CA, USA). Briefly, HEK293 cells or HEK293 Tet-On 3G Cells (Clontech, CA, USA) were cultured in Dulbecco's modified Eagle's medium supplemented with 10% Tet System Approved FBS (Clontech, CA, USA) and recommended concentration of antibiotics for selection (e.g. G413, puromycin, hygromycin B) or gene expression (doxycycline) in appropriate steps. Cells were transfected using Xfect Transfection Reagent (Clontech, CA, USA) according to the manufacturer's instructions.

Antibodies. The following primary antibodies were used: anti-tuberin (C-20) from Santa Cruz Biotechnology (Santa Cruz, CA, USA); anti-FLAG and anti-beta-actin from Sigma (MO, USA); and anti-beta-tubulin III (clone TuJ1) from Babco (CA, USA).

Immunoblotting. Protein concentration was determined using the DC-protein assay (Bio-Rad, CA, USA). Cells were lysed with Laemmli buffer and equal amounts of

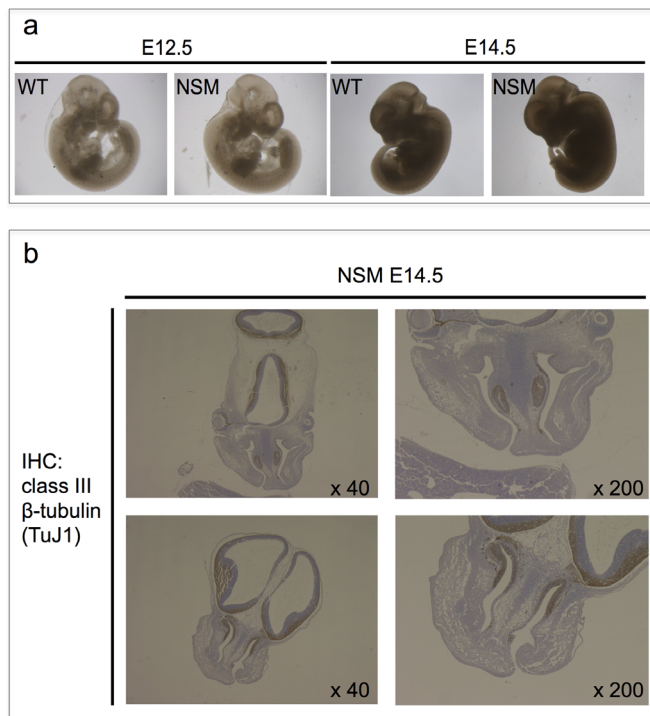


Figure 3 | Histological analysis of NSM Tg-positive embryos. (a) Macroscopic analysis of embryos. There were no apparent abnormalities or difference in size among individual embryos at any stage irrespective of their NSM Tg genetic status. (b) Class III beta-tubulin (TuJ1) immunohistochemical (IHC) analysis of embryonic tissue sections. Representative coronal sections of the embryo heads carrying NSM Tg are shown. Exencephaly, which is frequently associated with lethality in Eker homozygotes, was not observed.

protein were separated by standard SDS-PAGE, followed by transfer onto a PVDF membrane (Millipore, MA, USA). Blocking was performed with Odyssey blocking buffer (Li-Cor Biosciences, Lincoln, NE, USA). The primary antibody was applied in the same blocking solution, followed by incubation with a goat anti-rabbit or a goat anti-mouse Alexa Fluor 680 secondary antibody (Invitrogen, Carlsbad, CA, USA). Antibody binding was detected and quantified using the Odyssey system (Li-Cor Biosciences).

Immunofluorescence. Cells were plated in a glass-bottomed dish (Matsunami, Osaka, Japan) at a density of 1×10^4 cells/well, transfected as described above, and fixed and permeabilised in 2% paraformaldehyde and 0.1% Triton X-100 for 30 min at 4°C. Cells were then incubated with primary antibodies overnight at 4°C, followed by the secondary antibodies (Alexa Fluor 488-labelled anti-mouse IgG; Alexa Fluor 568-labelled anti-rabbit IgG, Invitrogen, CA, USA) and the DNA stain 4', 6-diamidino-2-phenylindole dihydrochloride (DAPI, Invitrogen) for 1 h at room-temperature. The stained cells were examined using a BZ-9000 fluorescence microscope (Keyence, Osaka, Japan).

Flow Cytometry. pTRE3G-ZsGreen1 vector, provided with the Tet-On 3G System kit (Clontech, CA, USA), was used to express ZsGreen simultaneously with the WT-, GSM-, or NSM-tuberin utilising the internal ribosome entry site (IRES) sequence according to the manufacturer's instructions. Single-cell suspensions were obtained by filtering through a 40- μ m filter. Cell sorting was performed on single-cell suspensions using an Epics Altra flow cytometer (Beckman Coulter, CA, USA). A sample flow was irradiated with a sapphire laser (wavelength: 488 nm), and the intensities of the forward scatter and fluorescence around 525 nm were collected (20,000 particles/sample). ZsGreen-positive cells were sorted at less than 700 events/s.

Animal studies and histological analyses. The animal experiments were performed in accordance with a protocol approved by Juntendo University, Tohoku University, and PhoenixBio Inc. Tissues from embryos were fixed in 10% buffered formalin, embedding in paraffin, sectioned, and routine histological examinations were performed after haematoxylin and eosin staining. For immunostaining, tissue sections were deparaffinised, preheated in 10 mM sodium citrate buffer (pH 6.0) in a microwave oven, and pretreated with 3% H₂O₂ solution for 10 min. Blocking was performed using 5% normal goat serum in wash buffer (1% BSA, Tris-buffered saline, 0.1% Tween 20, 0.07% NaN₃). Then, sections were incubated with the primary antibody (1/200 dilution in wash buffer) overnight at 4°C. Antibody binding was

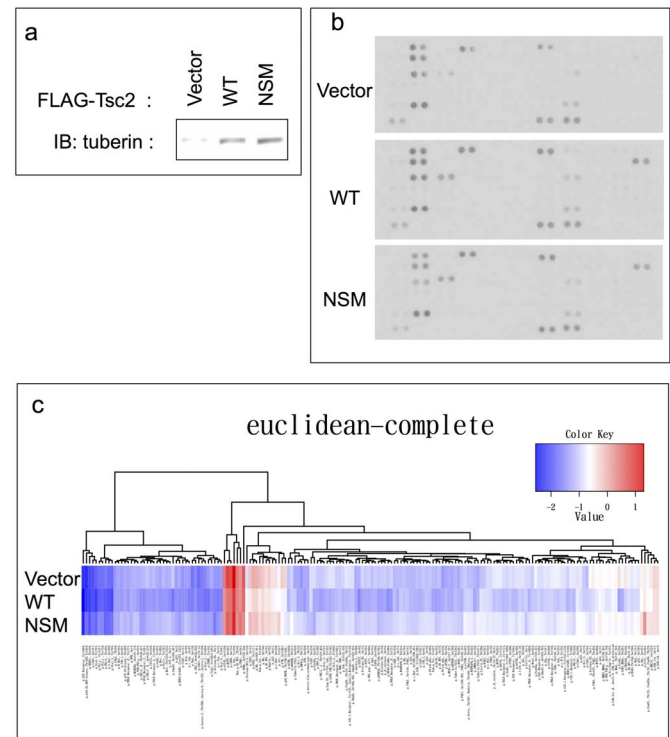


Figure 4 | Comprehensive analysis involving a variety of signal transduction molecules in transient expression of the tuberlin variants. (a) Transient expression of the tuberlin variants. HEK293 cells were transiently transfected with each expression vector plasmid and subjected to the following analyses. The blots have been cropped focusing on the bands of interest; See Supplementary Fig. S3 for full-length blots. (b) Phospho-Receptor Tyrosine Kinase (RTK) Array analysis. Levels of Phospho-RTK were assessed using a horseradish peroxidase-conjugated phospho-tyrosine antibody followed by chemiluminescence detection. No significant differences were observed in the relative tyrosine phosphorylation statuses of 44 different RTKs investigated in forced transient WT- or NSM-tuberin expressing cells. (c) Reverse Phase Protein Array (RPPA) analysis. The relative concentration values of the 180 anti-phospho antibody targets are represented as a heat map. No prominent differences were observed.

detected using the Envision system (DAKO, Glostrup, Denmark) using 3,3'-diaminobenzidine tetrahydrochloride (DAB; Dojindo, Kumamoto, Japan) as the substrate for peroxidase, followed by counterstaining with haematoxylin.

Phospho-Receptor Tyrosine Kinase (RTK) Array analysis. Phospho-RTK array analysis was performed using the Proteome Profiler Array Kit (R&D Systems, Minneapolis, MN, USA) according to the manufacturer's instructions. Briefly, transiently transfected HEK293 cells were lysed in the provided lysis buffer, incubated with the provided membrane, and RTKs were captured by antibodies spotted on a membrane. Then, levels of Phospho-RTK were assessed using a horseradish peroxidase-conjugated phospho-tyrosine antibody followed by chemiluminescence detection. This analysis allows simultaneous detection of relative tyrosine phosphorylation status of 44 different RTKs, which are listed in Supplementary Note S1.

Reverse Phase Protein Array (RPPA) analysis. RPPA analysis was performed by the Carna Biosciences assay service (Kobe, Japan) as previously described⁴⁴. Briefly, transiently transfected HEK293 cells were homogenised and prepared with RIPA buffer (Thermo Scientific, IL, USA) supplemented with phosphatase (Thermo Scientific) and protease inhibitor cocktails (Sigma). Serially diluted cell lysates (1:1, 1:2, 1:4, and 1:8) were spotted onto glass slides with an array in eight replicates. Signals from slides stained with anti-phospho antibodies were analysed with the SuperCurve algorithm⁴⁵ to obtain a single value of relative concentration for each lysate. The relative concentration values are represented as a heat map. The 180 targets of the anti-phospho antibodies utilised in this study are also shown in Supplementary Note S2.

- Gomez, M. R., Sampson, J. R. & Whittemore, V. H. *Tuberous Sclerosis Complex*. (Oxford University Press, 1999).



2. van Slechtenhorst, M. *et al.* Identification of the tuberous sclerosis gene TSC1 on chromosome 9q34. *Science* **277**, 805–808 (1997).
3. European Chromosome 16 Tuberous Sclerosis Consortium. Identification and characterization of the tuberous sclerosis gene on chromosome 16. *Cell* **75**, 1305–1315 (1993).
4. Manning, B. D. & Cantley, L. C. Rheb fills a GAP between TSC and TOR. *Trends Biochem. Sci.* **28**, 573–576 (2003).
5. Li, Y., Corradetti, M. N., Inoki, K. & Guan, K. L. TSC2: filling the GAP in the mTOR signaling pathway. *Trends Biochem. Sci.* **29**, 32–38 (2004).
6. Martin, D. E. & Hall, M. N. The expanding TOR signaling network. *Curr. Opin. Cell Biol.* **17**, 158–166 (2005).
7. Ma, X. M. & Blenis, J. Molecular mechanisms of mTOR-mediated translational control. *Nat. Rev. Mol. Cell Biol.* **10**, 307–318 (2009).
8. Niida, Y. *et al.* Analysis of both TSC1 and TSC2 for germline mutations in 126 unrelated patients with tuberous sclerosis. *Hum. Mutat.* **14**, 412–422 (1999).
9. Jones, A. C. *et al.* Comprehensive mutation analysis of TSC1 and TSC2-and phenotypic correlations in 150 families with tuberous sclerosis. *Am. J. Hum. Genet.* **64**, 1305–1315 (1999).
10. Dabora, S. L. *et al.* Mutational analysis in a cohort of 224 tuberous sclerosis patients indicates increased severity of TSC2, compared with TSC1, disease in multiple organs. *Am. J. Hum. Genet.* **68**, 64–80 (2001).
11. Maheshwar, M. M. *et al.* The GAP-related domain of tuberin, the product of the TSC2 gene, is a target for missense mutations in tuberous sclerosis. *Hum. Mol. Genet.* **6**, 1991–1996 (1997).
12. Jansen, A. C. *et al.* Unusually mild tuberous sclerosis phenotype is associated with TSC2 R905Q mutation. *Ann. Neurol.* **60**, 528–539 (2006).
13. Wentink, M. *et al.* Functional characterization of the TSC2 c.3598C>T (p.R1200W) missense mutation that co-segregates with tuberous sclerosis complex in mildly affected kindreds. *Clin. Genet.* **81**, 453–461 (2012).
14. Nellist, M. *et al.* Distinct effects of single amino-acid changes to tuberin on the function of the tuberin-hamartin complex. *Eur. J. Hum. Genet.* **13**, 59–68 (2005).
15. Mayer, K., Goedbloed, M., van Zijl, K., Nellist, M. & Rott, H. D. Characterisation of a novel TSC2 missense mutation in the GAP related domain associated with minimal clinical manifestations of tuberous sclerosis. *J. Med. Genet.* **41**, e64 (2004).
16. Nellist, M. *et al.* TSC2 missense mutations inhibit tuberin phosphorylation and prevent formation of the tuberin-hamartin complex. *Hum. Mol. Genet.* **10**, 2889–2898 (2001).
17. Shah, O. J. & Hunter, T. Critical role of T-loop and H-motif phosphorylation in the regulation of S6 kinase 1 by the tuberous sclerosis complex. *J. Biol. Chem.* **279**, 20816–20823 (2004).
18. Eker, R. & Mossige, J. A dominant gene for renal adenomas in the rat. *Nature* **189**, 858–859 (1961).
19. Yeung, R. S. *et al.* Predisposition to renal carcinoma in the Eker rat is determined by germ-line mutation of the tuberous sclerosis 2 (TSC2) gene. *Proc. Natl. Acad. Sci. U. S. A.* **91**, 11413–11416 (1994).
20. Hino, O. *et al.* The predisposing gene of the Eker rat inherited cancer syndrome is tightly linked to the tuberous sclerosis (TSC2) gene. *Biochem. Biophys. Res. Commun.* **203**, 1302–1308 (1994).
21. Kobayashi, T., Hirayama, Y., Kobayashi, E., Kubo, Y. & Hino, O. A germline insertion in the tuberous sclerosis (Tsc2) gene gives rise to the Eker rat model of dominantly inherited cancer. *Nat. Genet.* **9**, 70–74 (1995).
22. Kobayashi, T. *et al.* Transgenic rescue from embryonic lethality and renal carcinogenesis in the Eker rat model by introduction of a wild-type Tsc2 gene. *Proc. Natl. Acad. Sci. U. S. A.* **94**, 3990–3993 (1997).
23. Shiono, M. *et al.* The G1556S-type tuberin variant suppresses tumor formation in tuberous sclerosis 2 mutant (Eker) rats despite its deficiency in mTOR inhibition. *Oncogene* **27**, 6690–6697 (2008).
24. Momose, S. *et al.* Identification of the coding sequences responsible for Tsc2-mediated tumor suppression using a transgenic rat system. *Hum. Mol. Genet.* **11**, 2997–3006 (2002).
25. Hino, O. *et al.* Spontaneous and radiation-induced renal tumors in the Eker rat model of dominantly inherited cancer. *Proc. Natl. Acad. Sci. U. S. A.* **90**, 327–331 (1993).
26. Rennebeck, G. *et al.* Loss of function of the tuberous sclerosis 2 tumor suppressor gene results in embryonic lethality characterized by disrupted neuroepithelial growth and development. *Proc. Natl. Acad. Sci. U. S. A.* **95**, 15629–15634 (1998).
27. Kobayashi, T. *et al.* Renal carcinogenesis, hepatic hemangiomatosis, and embryonic lethality caused by a germ-line Tsc2 mutation in mice. *Cancer Res.* **59**, 1206–1211 (1999).
28. Kobayashi, T. *et al.* A germ-line Tsc1 mutation causes tumor development and embryonic lethality that are similar, but not identical to, those caused by Tsc2 mutation in mice. *Proc. Natl. Acad. Sci. U. S. A.* **98**, 8762–8767 (2001).
29. Lu, F. L., Hojo, M., Maluccio, M., Yamaji, K. & Suthanthiran, M. Rapamycin blocks tumor progression: unlinking immunosuppression from antitumor efficacy. *Transplantation* **73**, 1565–1572 (2002).
30. Meric-Bernstam, F. & Gonzalez-Angulo, A. M. Targeting the mTOR signaling network for cancer therapy. *J. Clin. Oncol.* **27**, 2278–2287 (2009).
31. Guba, M. *et al.* Rapamycin inhibits primary and metastatic tumor growth by antiangiogenesis: involvement of vascular endothelial growth factor. *Nat. Med.* **8**, 128–135 (2002).
32. Hudes, G. *et al.* Temsirolimus, interferon alfa, or both for advanced renal-cell carcinoma. *N. Engl. J. Med.* **356**, 2271–2281 (2007).
33. Atkins, M. B. *et al.* Randomized phase II study of multiple dose levels of CCI-779, a novel mammalian target of rapamycin kinase inhibitor, in patients with advanced refractory renal cell carcinoma. *J. Clin. Oncol.* **22**, 909–918 (2004).
34. Motzer, R. J. *et al.* Efficacy of everolimus in advanced renal cell carcinoma: a double-blind, randomised, placebo-controlled phase III trial. *Lancet* **372**, 449–456 (2008).
35. Yao, J. C. *et al.* Everolimus for advanced pancreatic neuroendocrine tumors. *N. Engl. J. Med.* **364**, 514–523 (2011).
36. Dutcher, J. P. Recent developments in the treatment of renal cell carcinoma. *Ther. Adv. Urol.* **5**, 338–353 (2013).
37. Abraham, R. T. Mammalian target of rapamycin: immunosuppressive drugs uncover a novel pathway of cytokine receptor signaling. *Curr. Opin. Immunol.* **10**, 330–336 (1998).
38. Kahan, B. D., Julian, B. A., Pescovitz, M. D., Vanrenterghem, Y. & Neylan, J. Sirolimus reduces the incidence of acute rejection episodes despite lower cyclosporine doses in caucasian recipients of mismatched primary renal allografts: a phase II trial. Rapamune Study Group. *Transplantation* **68**, 1526–1532 (1999).
39. Sehgal, S. N. Sirolimus: its discovery, biological properties, and mechanism of action. *Transplant. Proc.* **35**, 7S–14S (2003).
40. Krueger, D. A. *et al.* Everolimus for subependymal giant-cell astrocytomas in tuberous sclerosis. *N. Engl. J. Med.* **363**, 1801–1811 (2010).
41. Strizheva, G. D. *et al.* The spectrum of mutations in TSC1 and TSC2 in women with tuberous sclerosis and lymphangiomyomatosis. *Am. J. Respir. Crit. Care Med.* **163**, 253–258 (2001).
42. Khare, L. *et al.* A novel missense mutation in the GTPase activating protein homology region of TSC2 in two large families with tuberous sclerosis complex. *J. Med. Genet.* **38**, 347–349 (2001).
43. Hochi, S., Ninomiya, T., Waga-Homma, M., Sagara, J. & Yuki, A. Secretion of bovine alpha-lactalbumin into the milk of transgenic rats. *Mol. Reprod. Dev.* **33**, 160–164 (1992).
44. Masuda, M. *et al.* Alternative mTOR signal activation in sorafenib-resistant hepatocellular carcinoma cells revealed by array-based pathway profiling. *Mol. Cell. Proteomics*, [Epub ahead of print] (2014).
45. Tabus, I. *et al.* Nonlinear Modeling of Protein Expressions in Protein Arrays. *IEEE Transaction on Signal Processing* **54**, 2394–2407 (2006).

Acknowledgments

This research was supported by a Grant-in-aid for Cancer Research from the Ministry of Education, Culture, Sports, Science, and Technology of Japan. We thank M. Abe and Y. Sugiura for their technical assistance.

Author contributions

M.S. and T.K. designed the study; M.S., T.K. and R.T. performed experiments and analysed data; M.S. and T.K. wrote the manuscript; M.U., C.I. and O.H. gave technical support and conceptual advice.

Additional information

Supplementary information accompanies this paper at <http://www.nature.com/scientificreports>

Competing financial interests: The authors declare no competing financial interests.

How to cite this article: Shiono, M. *et al.* Transgenic expression of the N525S-tuberin variant in Tsc2 mutant (Eker) rats causes dominant embryonic lethality. *Sci. Rep.* **4**, 5927; DOI:10.1038/srep05927 (2014).



This work is licensed under a Creative Commons Attribution-NonCommercial-NoDerivs 4.0 International License. The images or other third party material in this article are included in the article's Creative Commons license, unless indicated otherwise in the credit line; if the material is not included under the Creative Commons license, users will need to obtain permission from the license holder in order to reproduce the material. To view a copy of this license, visit <http://creativecommons.org/licenses/by-nc-nd/4.0/>